International Journal of Adhesion & Adhesives 31 (2011) 666–673

Contents lists available at ScienceDirect

International Journal of Adhesion & Adhesives

journal homepage: www.elsevier.com/locate/ijadhadh

Tensile strength of two-part epoxy paste adhesives: Influence of mixing technique and micro-void formation

K.B. Katnam *, J.P.J. Stevenson, W.F. Stanley, M. Buggy, T.M. Young

Irish Centre for Composites Research (IComp), Materials Science and Surface Institute (MSSI), University of Limerick, Limerick, Ireland

ARTICLE INFO

Article history:
Accepted 12 June 2011
Available online 29 June 2011

Keywords:
Epoxy adhesives
Destructive testing
Microscopy
Mechanical properties of adhesives
X-ray microtomography

ABSTRACT

Two-part epoxy paste adhesives are frequently used to bond metals and composite materials in many structural applications. After mixing two reactive parts (by weight or volume ratio), adhesive paste is applied to the substrate surfaces and cured at elevated temperatures. Air-entrapment during mixing and/or application process often produces micro-voids in the adhesive bondlines and influences the strength of the bonded joints. In this work, void formation was investigated using two adhesive mixing techniques: (a) dual-cartridge and static-mixer with a dispenser and (b) hand-mix. Flat adhesive sheets were cured by mixing a two-part epoxy adhesive, and bulk specimens with notches were cut using CNC-machining. Using X-ray microtomography scans, the micro-voids were detected and material porosity was evaluated. Furthermore, tensile tests were performed on the specimens and two-dimensional digital image correlation (2D DIC) was employed to analyse the surface strain concentrations near the notches. The fracture surfaces were examined using optical and scanning electron microscopy. The results indicated that mixing technique influences the formation of micro-voids and thus the tensile strength of two-part epoxy paste adhesives.

1. Introduction

Adhesive usage is gaining momentum in structural applications for assembling both primary and secondary structural components. In the aircraft industry [1], the main use of structural adhesives is in bonding internal structural elements (*e.g.* stringers) to skins in fuselage, wing, aileron, *etc.* However, for the optimal performance of adhesive joints, the bonding process must overcome two major issues: (a) reliable adhesive application (*e.g.* mixing process and application of two-part paste adhesives) and (b) defect-free bondlines (*e.g.* kissing bonds and micro-voids). Micro-voids are frequently seen in adhesive bonds cured at elevated temperatures. Though the average size of these micro-voids is small ($<100\,\mu m$), the effective cross-sectional area of the bond reduces significantly with increase in void density and thus influences the structural performance. Void formation is often connected to: (a) air-entrapment during adhesive mixing and/or application, (b) vaporisation of the moisture absorbed by substrate surfaces (or by carrier in film adhesives) prior to bonding, (c) the type of substrate surface preparation, etc. [2–5].

The structural strength of bonded joints depends on the mechanical properties of substrate material, adhesive material and substrate–adhesive interface. To characterise the mechanical properties of adhesives, experimental tests are performed on either bulk specimens or bonded joints (*i.e.* in-situ form). It is often argued that the constraint-effect (bondline being constrained by two substrates) may influence the mechanical properties and thus the properties obtained through bulk material testing may not represent the in-situ properties. However, some research studies [6–9] showed that the mechanical behaviour of the bulk adhesive material is similar to those in bonded joints.

In this paper, a two-part paste adhesive was considered to investigate the influence of micro-voids on the tensile strength. Bulk specimens were manufactured using two different mixing techniques—to achieve two different porosity levels in the bulk material. The key objectives were: (a) to perform tensile tests on double-notched specimens and evaluate the influence of micro-voids on the tensile strength of two-part epoxy paste adhesives, (b) to monitor surface strains near the notches using 2D DIC for failure strains, (c) to evaluate the porosity levels in dispenser-mix and hand-mix specimens using X-ray microtomography and (d) to examine fracture surfaces using optical and scanning electron microscopy and identify failure mechanisms. The study indicated that adhesive micro-voids adversely affect the failure stresses and strains.

2. Materials and manufacturing

2.1. Two-part epoxy adhesive

A two-part epoxy paste adhesive, EA 9380.05 from Henkel Adhesives, was used to manufacture bulk specimens by curing thin

* Corresponding author. Tel.: +353 6120 2253; fax: +353 61 202944.
E-mail address: Kali-Babu.Katnam@ul.ie (K.B. Katnam).

0143-7496/$ - see front matter © 2011 Elsevier Ltd. All rights reserved.
doi:10.1016/j.ijadhadh.2011.06.005

sheets. It is a toughened structural adhesive with glass particles to improve fracture properties. This adhesive was supplied in both dual cartridge and tin forms. For the current study, dispenser-mix and hand-mix techniques were employed to manufacture bulk adhesive sheets. The process used for dispenser-mix is shown in Fig. 1. The dispenser was loaded with a dual cartridge and a static mixer, and compressed air was pumped into the system to get a uniform adhesive paste from the nozzle of the static mixer. For hand-mix adhesive, the two parts were weighed and mixed in a bowl using a rod/spatula until a uniform colour is obtained.

2.2. Adhesive application and curing

To manufacture bulk adhesive sheets two PTFE sheets were used to sandwich the adhesive paste, and then two aluminium plates were used to apply pressure on the PTFE-adhesive sandwich system. For the dispenser-mix, the adhesive was applied on to one of the PTFE sheets by beading the paste adhesive from the nozzle. On the other hand, for the hand-mix case, adhesive paste was applied in the middle of the PTFE sheet and then spread using a spatula (by moving the spatula in only one direction). Once the adhesive was applied, the PTFE-adhesive sandwich system was enclosed using the aluminium plates. The thickness of the adhesive sheet was controlled by inserting brass shims (1 mm) on the four edges (located using a high temperature tape) of the PTFE sheets. The adhesive was then cured in a hot drape former (HDF2 from Laminating Technology) for 4 h at 80 °C under 10 kPA pressure.

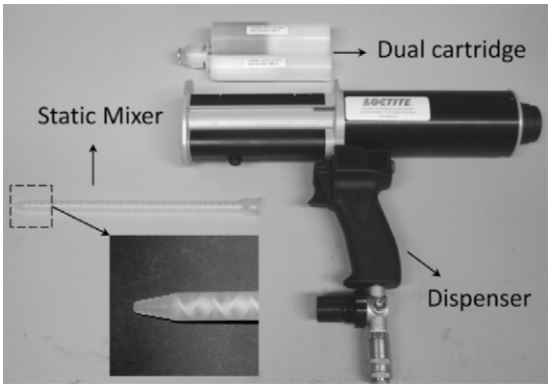

Fig. 1. Dispenser-mix using dual-cartridge and static-mixer.

2.3. Bulk specimens

Bulk specimens were manufactured by cutting the cured adhesive sheets using a CNC machine. The dimensional details (in mm) of the bulk specimens are shown in Fig. 2a. The thickness of the specimens, *t*, is 1 mm. To induce strain concentration and fracture in the middle of the specimen, a circular notch with 5 mm radius was cut on both edges. The specimen geometry (with two circular notches) is used to monitor strain concentrations at failure using the 2D digital image correlation technique. However, the notch geometry used (which is not a sharp notch) introduces negligible transverse stresses near the notch tip and thus the failure is predominantly governed by the axial stresses. The edge quality obtained from CNC-cutting is shown is Fig. 2b. Two circular holes (4 mm radius) were also drilled at the top and bottom for applying a tensile load using dowel pins to eliminate issues related to specimen alignment. To avoid failure at these pin holes, aluminium shims (1 mm) with holes are bonded with Loctite super glue on both sides.

3. Experimental work

3.1. Test setup

Tensile tests were conducted on bulk specimens in a Tinius-Olsen mechanical test machine with a 1000 N capacity load cell. The specimens were tested at three different crosshead displacement rates. Dowel pins were employed to accurately align the specimens and also to transfer the crosshead displacement. For each combination of mixing technique and displacement rate 3 tests were conducted, and axial load and crosshead displacement data were obtained. However, to accurately monitor the failure behaviour, one instrumented test was performed for each combination of mixing technique and displacement rate using a 2D DIC [10].

3.2. Digital image correlation

To experimentally evaluate the tangential-surface strains (*e.g.* axial strain, ε_{yy}), non-contact techniques such as 2D DIC gained popularity for material testing in recent times [11,12]. In the current study, the 2D DIC system was used to assess the surface strain evolution at the notches with increasing loads. To perform 2D DIC on the bulk specimens: (a) a random surface

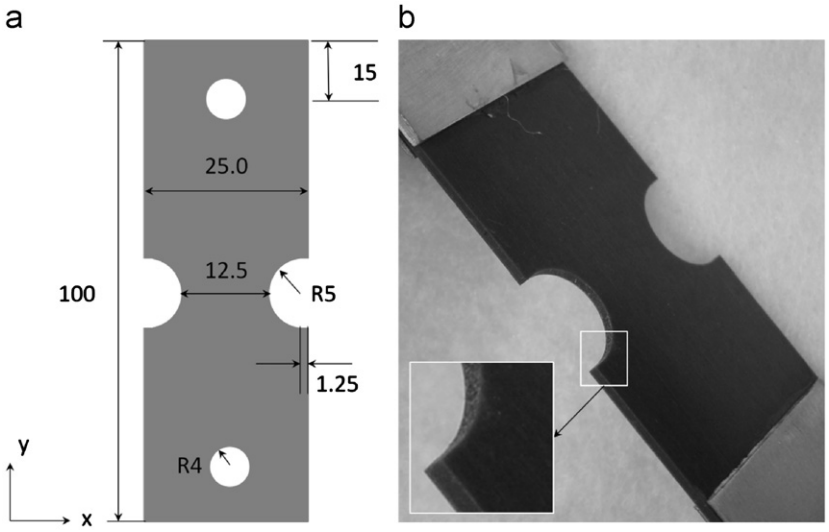

Fig. 2. Bulk specimen: (a) dimensions (in mm) and (b) the edge quality from CNC-cutting.

pattern is required and (b) the random pattern has to adhere to the specimen surface during the loading conditions. Moreover, for strain-gradients, smaller speckles give higher spatial resolution. To achieve the two aspects, the bulk specimen surfaces were speckled with Simoniz acrylic sprays (white and black). As the speckle distribution and their size (relative to the surface area being monitored) were vital for processing the digital images, the acrylic sprays were applied carefully to achieve a random as well as isotropic distribution, with speckle size between 30–300 μm (assessed using an optical microscope). The 2D DIC system was calibrated using the well-defined dimension (width, 25 mm) of the specimen, and processed to evaluate the tangential deformations and strains (see Section 4 for results).

3.3. Rate-dependent tests

It is known that bonded joints often manifest the intrinsic rate-dependent behaviour of adhesive materials [13–15]. To investigate the influence of micro-voids on rate-dependency, tensile tests were conducted at three different rates—with a hundred fold increase (0.1, 1.0 and 10.0 mm/min). The strain distributions near the two notches were obtained for each test rate using the 2D DIC (see Section 4 for results).

3.4. X-ray microtomography

To non-destructively evaluate the specimen quality obtained from the hot drape former, X-ray microtomography (Phoenix|X-ray nanotom by GE Sensing and Inspection Technologies) was employed to scan dispenser-mix and hand-mix representative specimens. The specimens were mounted on a rotatable specimen holder, which is between an X-ray source and a detector, and were scanned using a cone beam X-ray radiation (at 100 μA current, 80 kV voltage with 5 μm voxel size). Rotating the specimen by 360° degrees, a series of 2D images were taken to reconstruct a 3D image. Furthermore, porosity and particle analyses were performed to evaluate micro-void and particle content in dispenser-mix and hand-mix specimens (see Section 4 for results).

3.5. Fractography

The fracture surfaces were examined using SEM (JCM 5700 Carry Scope) for micro-voids to qualitatively assess their size and distribution. To avoid charge accumulation, the fracture surfaces were coated with gold (10 nm) before the fractographic observations. Both the dispenser-mix and hand-mix specimen fracture surfaces (obtained for 10.0 mm/min displacement rate) were examined (see Section 4 for results).

4. Results and discussion

In this section, the experimental data obtained are presented. The specimen void content, failure loads and strain distributions near the notches and surface micrographs are discussed.

4.1. Void content

X-ray microtomography scans on dispenser-mix and hand-mix representative specimens using cone beam radiation (at 100 μA current, 80 kV voltage with 5 μm voxel size) revealed micro-void formation and provided the micro-void content. The volume scanned and cross-sectional views obtained for a hand-mix specimen are shown in Fig. 3. The black patches in the bulk material represent volume with a density equal to air and thus micro-voids. Furthermore, porosity analyses were performed to evaluate

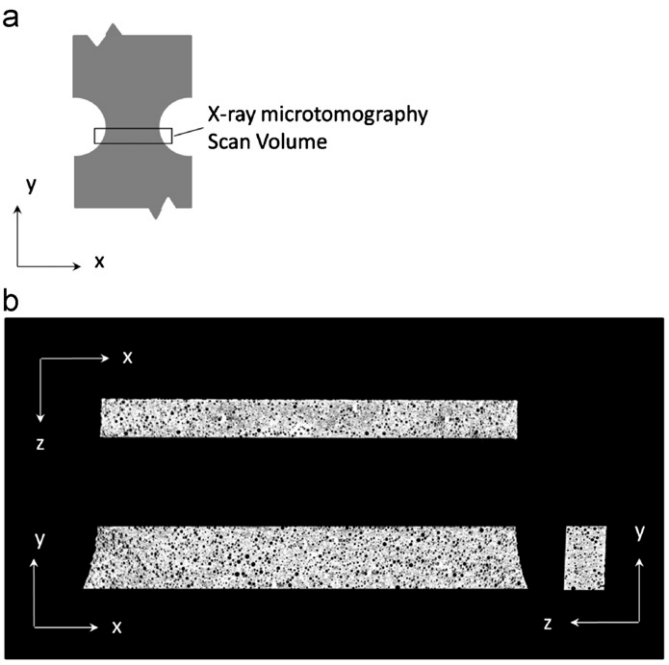

Fig. 3. X-ray microtomography on a hand-mix specimen: (a) a schematic showing the scanned volume and (b) the three cross-sectional views.

Table 1
X-ray microtomography scans on bulk specimens for estimating void and toughening particle content.

Specimen	Analysed volume (mm^3)	Void content (%)	Particle content (%)
Dispenser-mix	45.59	2.96	0.246
Hand-mix	25.56	13.42	0.259

micro-void content in dispenser-mix and hand-mix specimens and the results are given in Table 1. The porosity of the hand-mix specimen (13.42%) was nearly 3.5 times higher than the porosity of the dispenser-mix specimen (2.96%). Similarly, the particle contents were obtained for dispenser-mix and hand-mix specimens and found to be approximately 0.25% by volume (see Table 1).

4.2. Failure loads

Tensile tests were performed at three different displacement rates (0.1, 1.0 and 10.0 mm/min) and the failure loads obtained were compared for dispenser-mix and hand-mix specimens, see in Fig. 4. The specimens from dispenser-mix failed at higher loads with increased displacement rates, showing rate-dependency. However, the hand-mix specimens showed no rate-dependency. This rate-dependent behaviour was further examined using the 2D DIC technique.

4.3. Failure strains

The failure strains near the notches were evaluated from the specimens that were tested with the 2D DIC system. The width of the specimen was used to calibrate 2D DIC and it was found that the size of each pixel was approximately 40 μm. A facet size of 16×16 pixels was used in the analysis of the images for better spatial resolution as strain gradients exist near the notches.

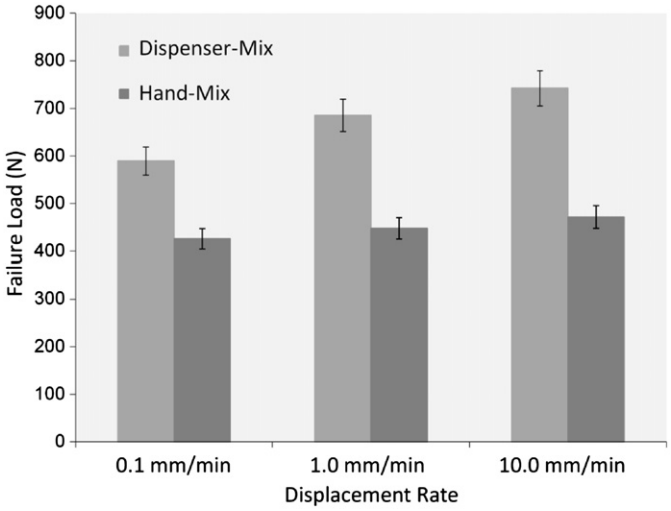

Fig. 4. Comparison of failure loads for dispenser-mix and hand-mix specimens.

A rectangular mask in the middle of the specimen (with 12.5 mm width) was used to process the digital images, and the axial-displacements and axial-strains were analysed.

First, the dispenser-mix specimens that were tested at 0.1, 1.0 and 10.0 mm/min rates were processed, and the contour plots for axial-displacement (U_y) and axial-strain (ε_{yy}) are shown in Fig. 5. Furthermore, the axial-strain profiles across the two notches were plotted at different loads and shown in Fig. 6 for 0.1, 1.0 and 10.0 mm/min rates. The axial-strain evolution with increased loads shows that strain concentrations exist near the notch tips. The strain profiles were symmetric at lower loads and became unsymmetric before failure. Similarly, for the hand-mix, the specimens tested at 0.1, 1.0 and 10.0 mm/min rates were analysed, and the contour plots for axial-displacement and axial-strain are shown in Fig. 7. The axial-strain profiles across the two notches were plotted at different loads and shown in Fig. 8 for 0.1, 1.0 and 10.0 mm/min rates.

The experimental data (Figs. 5–8) shows that the failure axial-displacements and axial-strains are sensitive to the adhesive mixing technique. The hand-mix specimens failed at relatively lower axial-displacements and axial-strains at the notch tip. The average failure axial-stresses and peak axial-strains for the dispenser-mix and hand-mix are given in Table 2. The average failure axial-stresses increased from 48.32 to 60.56 MPa (25.3% increase) when the displacement rate was increased from 0.1 to 10.0 mm/min (100 fold increase). However, the peak failure axial-strains, which were obtained from the peaks of unsymmetric strain profiles at failure from Fig. 6, are between 3.57–4.62% for the three rates. It is speculated that the material inhomogeneity, caused by adhesive mixing and micro-voids, causes the unsymmetric strain distribution and scatter in local strain values. For the hand-mix specimens, the average failure stress is nearly constant ($\approx$ 33 MPa) at the three rates. The peak failure axial-strains, obtained from Fig. 8, are between 1.87–2.54% for the three test rates. The size and number of micro-voids present in the material may have reduced the effective cross-sectional area and also caused local (at a micro scale) stress concentrations to promote failure at lower stress/strains when compared to the dispenser-mix material.

4.4. Failure surfaces

The fracture surfaces obtained from the dispenser-mix and hand-mix specimen, which were tested at 10.0 mm/min, were examined using optical and scanning electron microscopy. The area examined near the notch tip for the specimen is shown in Fig. 9a, and the optical micrographs are shown in Fig. 9b and c. Furthermore, the SEM micrographs obtained near the notch tip for the dispenser-mix specimen are shown in Fig. 10. For the hand-mix specimen, the SEM micrographs obtained are shown in Fig. 11. It was observed that the micro-voids found on the dispenser-mix fracture surface were comparatively less than on the hand-mix fracture surface. The majority of the micro-voids in the dispenser-mix fracture surface was between 5 and 20 μm in size; whereas for the hand-mix, it was between 20 and 100 μm. However, the fracture pattern around a micro-void or a particle in both dispenser-mix and hand-mix material was found to be very similar (see Figs. 10 and 11 at 2500 × magnification).

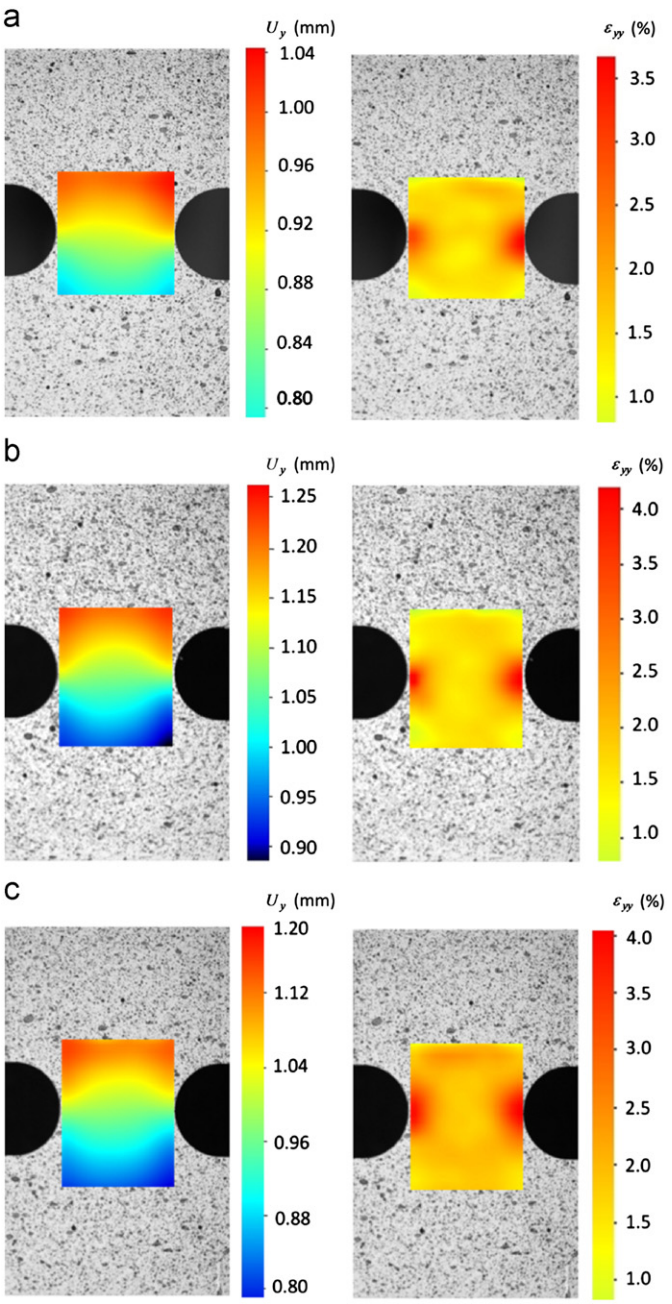

Fig. 5. Axial-displacement and axial-strain contour plots (just before failure) from the 2D DIC for the dispenser-mix specimens tested: (a) at 0.1 mm/min rate, (b) at 1.0 mm/min rate and (c) 10.0 m/min rate.

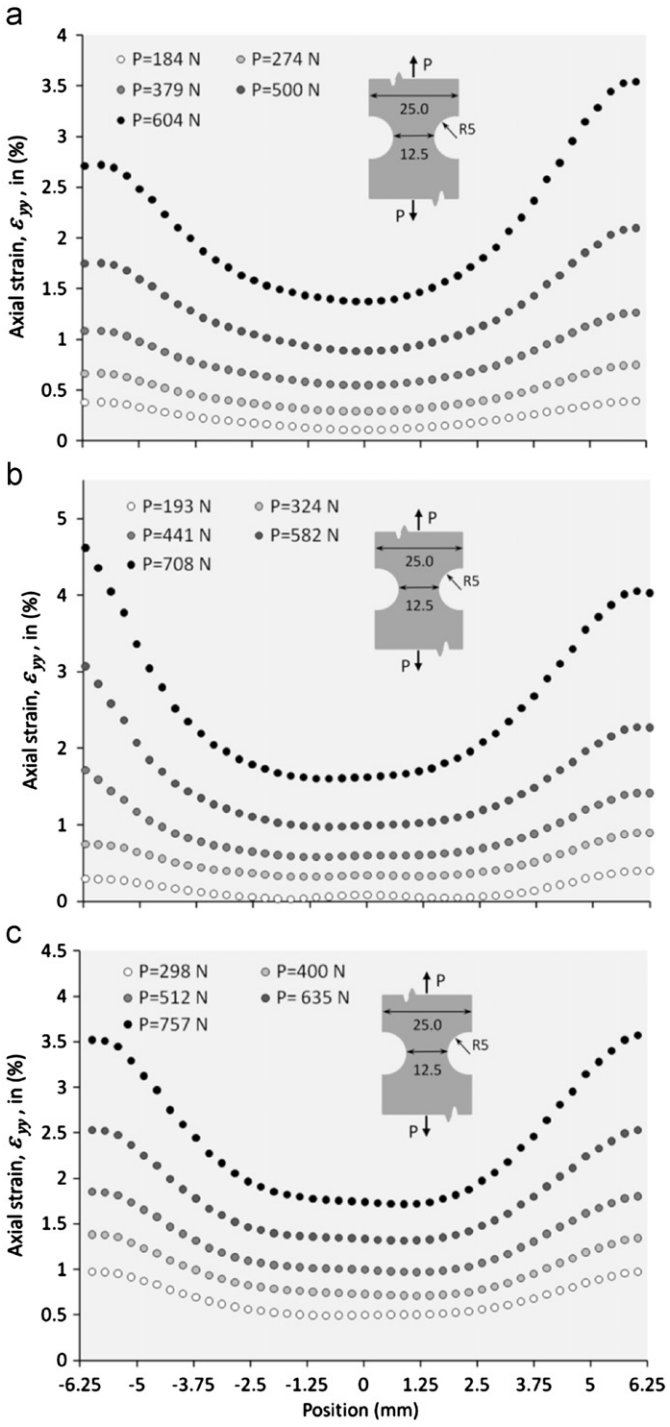

Fig. 6. Axial-strain profiles across the two notches for the dispenser-mix specimens tested as a function of applied load: (a) at 0.1 mm/min rate, (b) at 1.0 mm/min rate and (c) at 10.0 mm/min rate.

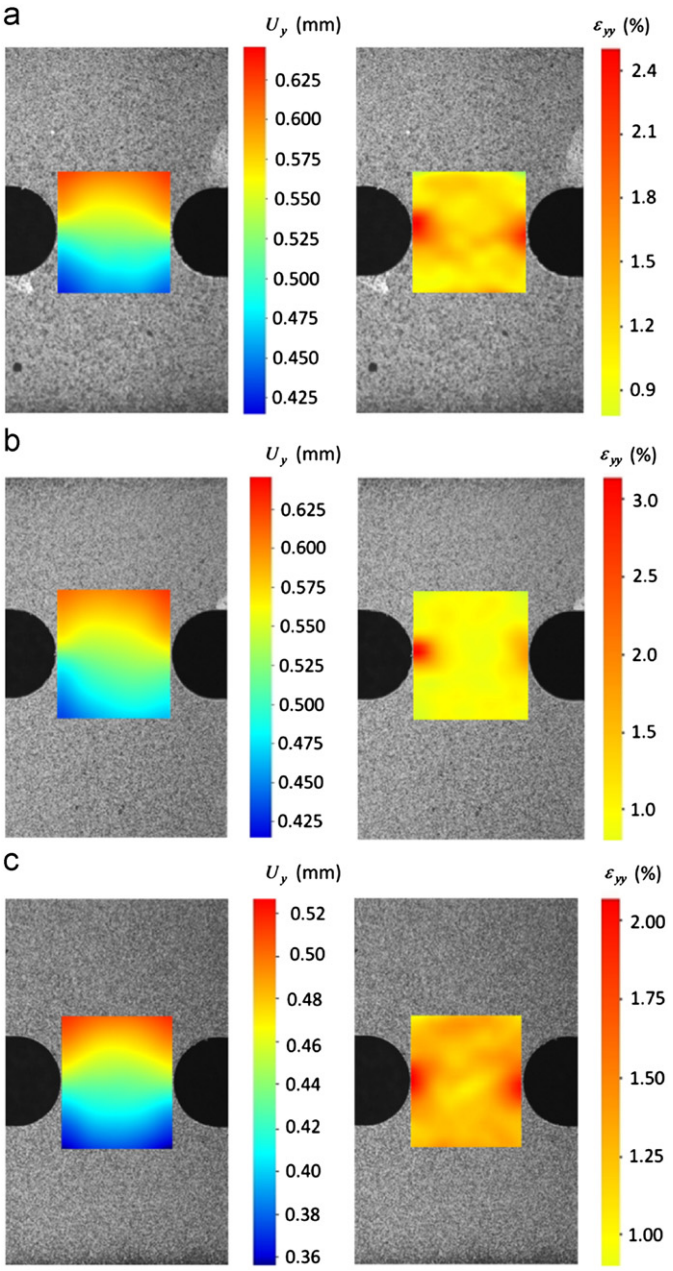

Fig. 7. Axial-displacement and axial-strain contour plots (just before failure) from the 2D DIC for the hand-mix specimens tested: (a) at 0.1 mm/min rate, (b) at 1.0 mm/min rate and (c) 10.0 mm/min rate.

5. Conclusions

A two-part epoxy paste adhesive (Hysol EA 9380.05) was used to investigate the influence of the mixing technique (dispenser-mix and hand-mix) and micro-void formation on the bulk tensile strength. Bulk adhesive sheets were manufactured using PTFE sheets as release agents between two aluminium plates and then test specimens with notches were cut from the cured sheets using CNC-machining. Tensile tests were conducted at three different displacement rates and the 2D DIC technique was employed to measure the strain gradients near the notches in both dispenser-mix and hand-mix specimens. The following observations were made:

- Bulk adhesive sheets of two-part epoxy paste adhesives can be manufactured using PTFE as a release agent, and test specimens with notches can be cut from the cured adhesive sheets using CNC-machining (see Fig. 2).
- Bulk specimens were scanned using X-ray microtomography. Micro-voids and toughening particles were successfully detected and their content was evaluated. This shows that X-ray microtomography may in general be used as a non-destructive technique to identify the bondline quality in bonded joints.
- For EA 9380.05, the tensile strength depends on the mixing technique and micro-voids. The dispenser-mix specimens

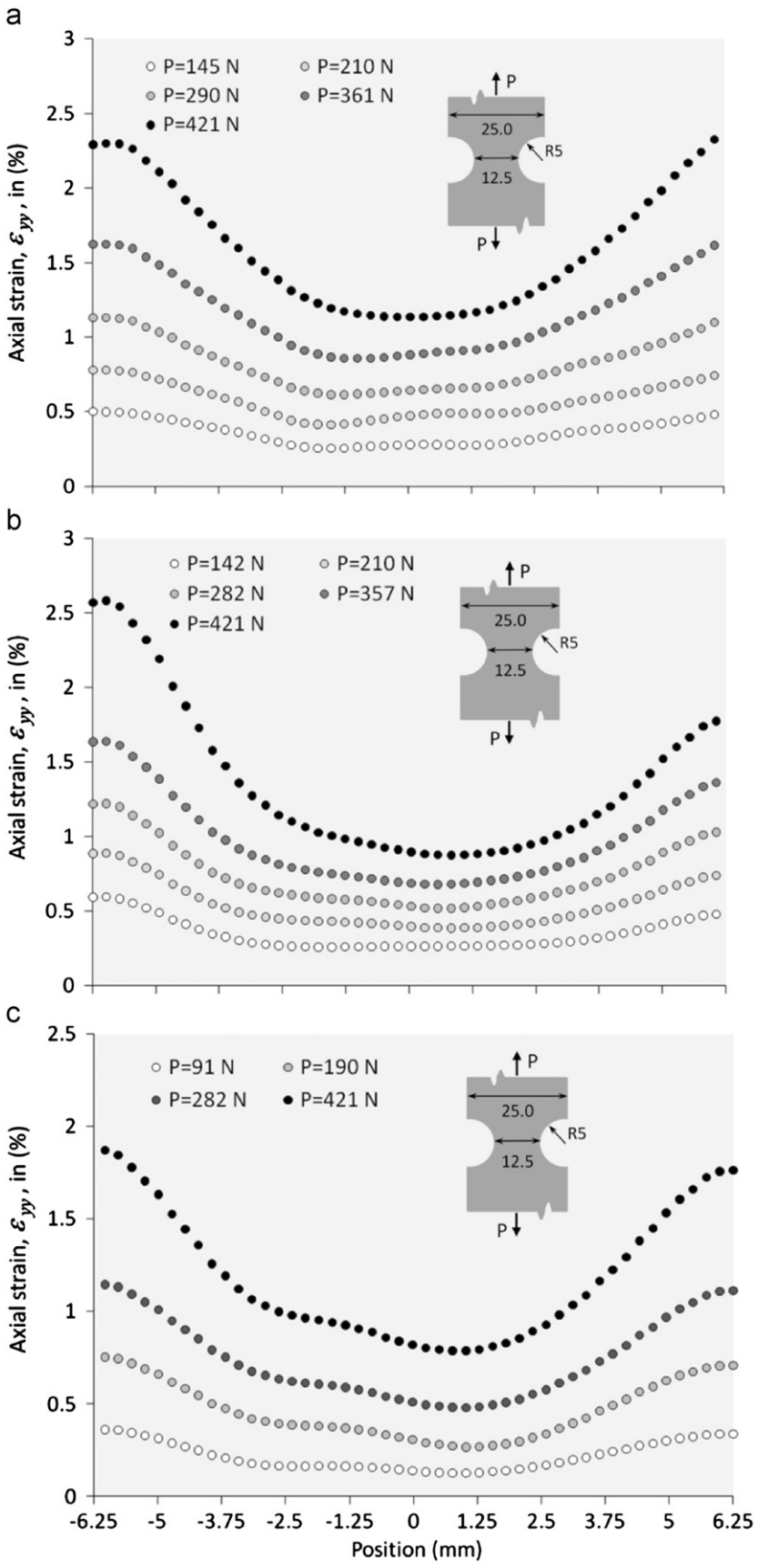

Fig. 8. Axial-strain profiles across the two notches for the hand-mix specimens tested as a function of applied load: (a) at 0.1 mm/min rate, (b) at 1.0 mm/min rate and (c) at 10.0 mm/min rate.

Table 2
Comparison of failure stresses and strains from dispenser-mix and hand-mix.

Mixing technique	Displacement rate (mm/min)	Failure		Variation (%)	
		σ_{avg} (MPa)[a]	ε_{max} (%)[b]	σ_{avg}	ε_{max}
Dispenser-mix	0.1	48.32	3.58	–	–
	1.0	56.64	4.62	+17.22	+29.05
	10.0	60.56	3.57	+25.33	−0.28
Hand-mix	0.1	33.72	2.36	−30.21	−34.08
	1.0	33.80	2.54	−30.05	−29.06
	10.0	33.71	1.87	−30.23	−47.76

[a] σ_{avg}: average stress at failure.
[b] ε_{max}: peak failure strain at the notches.

failed at considerably higher average stresses (> 30%) than the hand-mix specimens (see Fig. 4 and Table 2).
- The dispenser-mix specimens (with smaller and lesser number of micro-voids) failed at higher loads with increased displacement rates, whereas the hand-mix specimens (with larger and higher number of micro-voids) showed no rate-dependent behaviour (see Fig. 4).
- The near-notch strain gradients were measured using 2D DIC and it was observed that the failure strains of the dispenser-mix specimens, in general, were considerably higher than the failure strains of the hand-mix specimens (see Figs. 5–8).
- Detailed experimental and numerical studies, from a micro-mechanical viewpoint, are needed to thoroughly understand the influence of micro-voids on the failure behaviour of adhesively bonded joints.

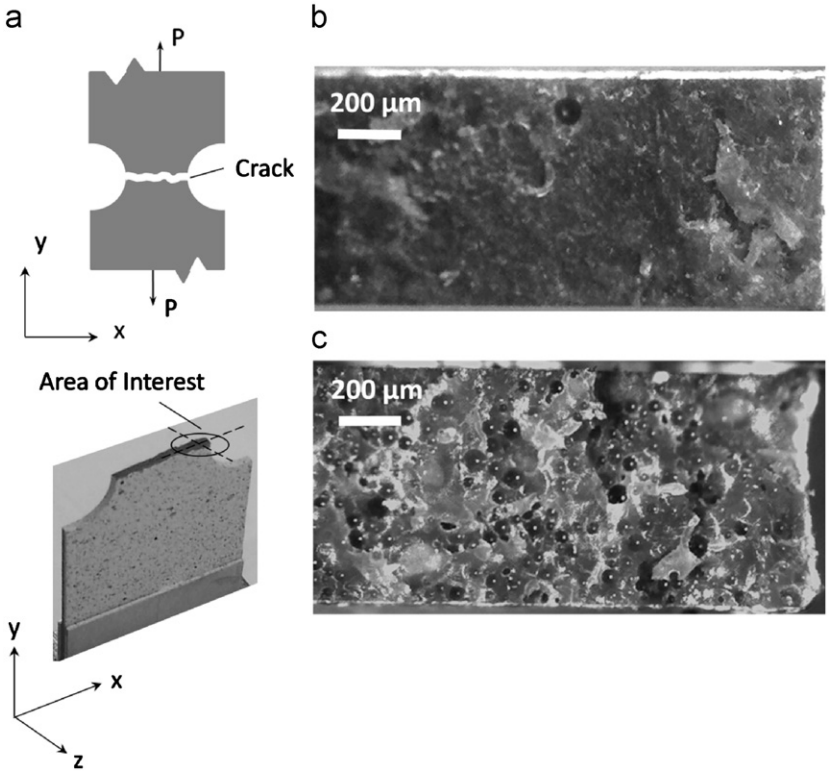

Fig. 9. Fracture surface examination: (a) area of interest (b) optical micrograph from the dispenser-mix specimen and (c) micrograph from the hand-mix specimen.

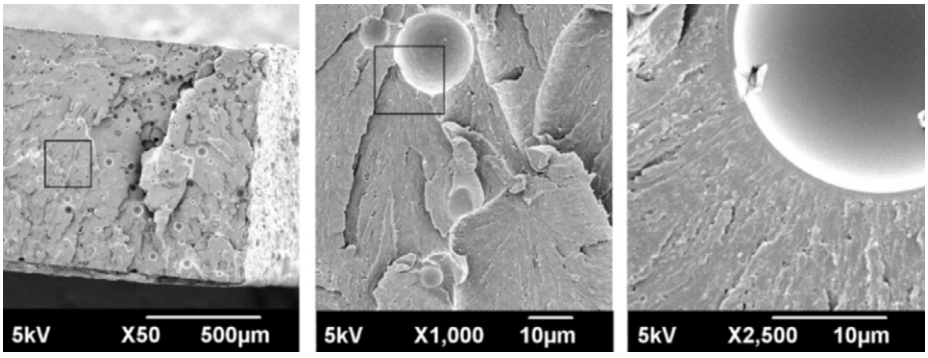

Fig. 10. Fracture surface examination of the dispenser-mix specimens at ×50, ×100, ×1000 and ×2500 magnifications.

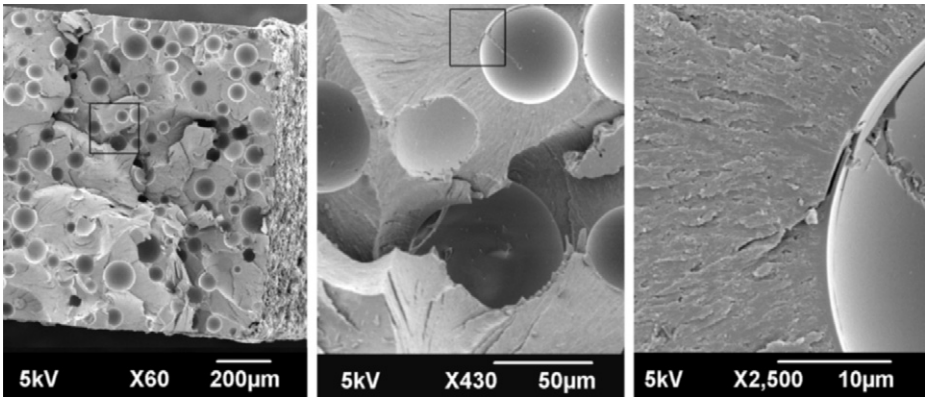

Fig. 11. Fracture surface examination of the hand-mix specimens at ×60, ×130, ×430 and ×2500 magnifications.

Acknowledgments

The authors would like to acknowledge (a) Enterprise Ireland for Research funding, (b) Henkel Adhesives for providing EA 9380.05 and dispenser-mix tools and (c) Dr. Calum Dickinson, Dr. Anthony Comer and Dr. Andrea Spaggiari at Materials Surface Science Institute at the University of Limerick for their useful suggestions.

References

[1] Higgins A. Adhesive bonding of aircraft structures. Int J Adhes Adhes 2000;20(5):367–76.
[2] Chester RJ, Roberts JD. Void minimization in adhesive joints. Int J Adhes Adhes 1989;9(3):129–38.
[3] Pearce PJ, Arnott DR, Camilleri A, Kindermann MR, Mathys GI, Wilson AR. Cause and effect of void formation during vacuum bag curing of epoxy film adhesives. J Adhes Sci Technol 1998;12(6):567–84.
[4] da Silva LFM, Adams RD, Gibbs M. Manufacture of adhesive joints and bulk specimens with high-temperature adhesives. Int J Adhes Adhes 2004;24(1):69–83.
[5] Bascom WD, Cottington RL. Air entrapment in use of structural adhesive films. J Adhes 1972;4(3):193–209.
[6] Lilleheden L. Mechanical properties of adhesives in situ and in bulk. Int J Adhes Adhes 1994;14(1):31–7.
[7] Jeandrau JP. Intrinsic mechanical characterization of structural adhesives. Int J Adhes Adhes 1986;6(4):229–31.
[8] Lees DE, Hutchinson AR. Mechanical characteristics of some cold-cured structural adhesives. Int J Adhes Adhes 1992;12(3):197–205.
[9] Zheng S, Ashcroft IA. A depth sensing indentation study of the hardness and modulus of adhesives. Int J Adhes Adhes 2005;25(1):67–76.
[10] StrainMaster, LaVision GmbH, 2010, 〈http://www.lavision.de〉.
[11] Pan B, Qian K, Xie H, Asundi A. Two-dimensional digital image correlation for in-plane displacement and strain measurement: a review. Meas Sci Technol 2009;20:17.
[12] Lagattu F, Brillaud J, Lafarie-Frenot M. High strain gradient measurements by using digital image correlation technique. Mater Charact 2004;53:17–28.
[13] Crocombe AD. Modelling and predicting the effects of test speed on the strength of joints made with FM73 adhesive. Int J Adhes Adhes 1995;15(1):21–7.
[14] Xu CC, Siegmund T, Ramani K. Rate-dependent crack growth in adhesives - II. Experiments and analysis. Int J Adhes Adhes 2003;23(1):15–22.
[15] Zgoul M, Crocombe AD. Numerical modelling of lap joints bonded with a rate-dependent adhesive. Int J Adhes Adhes 2004;24(4):355–66.